J|A|C|S ARTICLES

Published on Web 01/05/2010

Combined Single-Molecule Photon-Stamping Spectroscopy and Femtosecond Transient Absorption Spectroscopy Studies of Interfacial Electron Transfer Dynamics

Lijun Guo, Yuanmin Wang, and H. Peter Lu*

Center for Photochemical Sciences, Department of Chemistry, Bowling Green State University, Bowling Green, Ohio 43403

Received October 28, 2009; E-mail: hplu@bgsu.edu

Abstract: The inhomogeneous interfacial electron transfer (IET) dynamics of 9-phenyl-2,3,7-trihydroxy-6-fluorone (PF)-sensitized TiO_2 nanoparticles (NPs) has been probed by a single-molecule photon-stamping technique as well as ensemble-averaged femtosecond transient absorption spectroscopy. The forward electron transfer (FET) time shows a broad distribution at the single-molecule level, indicating the inhomogeneous interactions and ET reactivity of the PF/TiO_2 NP system. The broad distribution of the FET time is measured to be 0.4 ± 0.1 ps in the transient absorption and picoseconds to nanoseconds in the photon-stamping measurements. The charge recombination time, having a broad distribution at the single-molecule level, clearly shows a biexponential dynamic behavior in the transient absorption: a fast component of 3.0 ± 0.1 ps and a slow component of 11.5 ± 0.5 ns. We suggest that both strong and weak interactions between PF and TiO_2 coexist, and we have proposed two mechanisms to interpret the observed IET dynamics. A single-molecule photon-stamping technique and ensemble-averaged transient absorption spectroscopy provide efficient "zoom-in" and "zoom-out" approaches for probing the IET dynamics. The physical nature of the observed multiexponential or stretched-exponential ET dynamics in the ensemble-averaged experiments, often associated with dynamic and static inhomogeneous ET dynamics, can be identified and analyzed by single-molecule spectroscopy measurements.

Introduction

Dye-sensitized systems based on semiconductor nanomaterials, such as TiO_2,[1−27] SnO_2,[19,28,29] and ZrO_2,[24,27,30–32] have attracted significant interest in the past decades due to their potential applications in solar energy conversion,[2,21,33–35] photocatalysis,[26,36–38] and molecular devices.[39–42] At the dye/semiconductor surfaces, due to the energy difference between the lowest unoccupied molecular orbital (LUMO) of the dye molecule and the conduction band or the surface states of the semiconductors, electron transfer occurs at the interface within femtoseconds to hundreds of picoseconds.[1,2,6,8,10,11,13,43] Following a forward electron transfer (FET) process, a backward electron transfer (BET) event takes place within sub-nanoseconds to milliseconds after the electron is injected, involving possibly trapping and detrapping, non-Brownian diffusion, and scattering in the bulk of the semiconductor.[2,8,13,23,43] Often, complex ET dynamics is observed for the FET and BET processes, and the physical origins of the complex dynamics are typically difficult to identify by using ensemble-averaged experimental approaches alone.[44–56] The difficulty comes from both spatial and temporal inhomogeneities, which can be identified, measured, and analyzed by studying specific

(1) Abuabara, S. G.; Rego, L. G. C.; Batista, V. S. *J. Am. Chem. Soc.* **2005**, *127*, 18234–18242.
(2) Biju, V.; Micic, M.; Hu, D. H.; Lu, H. P. *J. Am. Chem. Soc.* **2004**, *126*, 9374–9381.
(3) De Angelis, F.; Fantacci, S.; Selloni, A.; Nazeeruddin, M. K.; Grätzel, M. *J. Am. Chem. Soc.* **2007**, *129*, 14156–14157.
(4) Duncan, W. R.; Prezhdo, O. V. *Annu. Rev. Phys. Chem.* **2007**, *58*, 143–184.
(5) Harris, J. A.; Trotter, K.; Brunschwig, B. S. *J. Phys. Chem. B* **2007**, *111*, 6695–6702.
(6) Kondov, I.; Čižek, M.; Benesch, C.; Wang, H. B.; Thoss, M. *J. Phys. Chem. C* **2007**, *111*, 11970–11981.
(7) Kondov, I.; Thoss, M.; Wang, H. B. *J. Phys. Chem. A* **2006**, *110*, 1364–1374.
(8) Pan, J.; Benkö, G.; Xu, Y. H.; Pascher, T.; Sun, L. C.; Sundström, V.; Polivka, T. *J. Am. Chem. Soc.* **2002**, *124*, 13949–13957.
(9) Ramakrishna, G.; Ghosh, H. N.; Singh, A. K.; Palit, D. K.; Mittal, J. P. *J. Phys. Chem. B* **2001**, *105*, 12786–12796.
(10) Ramakrishna, G.; Singh, A. K.; Palit, D. K.; Ghosh, H. N. *J. Phys. Chem. B* **2004**, *108*, 4775–4783.
(11) Ramakrishna, G.; Verma, S.; Jose, D. A.; Kumar, D. K.; Das, A.; Palit, D. K.; Ghosh, H. N. *J. Phys. Chem. B* **2006**, *110*, 9012–9021.
(43) Matylitsky, V. V.; Lenz, M. O.; Wachtveitl, J. *J. Phys. Chem. B* **2006**, *110*, 8372–8379.
(12) Robel, I.; Kuno, M.; Kamat, P. V. *J. Am. Chem. Soc.* **2007**, *129*, 4136–4137.
(13) She, C. X.; Guo, J. C.; Irle, S.; Morokuma, K.; Mohler, D. L.; Zabri, H.; Odobel, F.; Youm, K. T.; Liu, F.; Hupp, J. T.; Lian, T. *J. Phys. Chem. A* **2007**, *111*, 6832–6842.
(14) Wang, Y. M.; Wang, X. F.; Ghosh, S. K.; Lu, H. P. *J. Am. Chem. Soc.* **2009**, *131*, 1479–1487.
(15) Zhang, H. P.; Zhou, Y. L.; Zhang, M. H.; Shen, T.; Li, Y. L.; Zhu, D. B. *J. Phys. Chem. B* **2002**, *106*, 9597–9603.
(16) Ardo, S.; Meyer, G. J. *Chem. Soc. Rev.* **2009**, *38*, 115–164.
(17) Benkö, G.; Hilgendorff, M.; Yartsev, A. P.; Sundström, V. *J. Phys. Chem. B* **2001**, *105*, 967–974.
(18) Ghosh, H. N. *J. Chem. Sci.* **2007**, *119*, 205–215.
(19) Green, A. N. M.; Palomares, E.; Haque, S. A.; Kroon, J. M.; Durrant, J. R. *J. Phys. Chem. B* **2005**, *109*, 12525–12533.
(20) Kaniyankandy, S.; Verma, S.; Mondal, J. A.; Palit, D. K.; Ghosh, H. N. *J. Phys. Chem. C* **2009**, *113*, 3593–3594.
(21) O'Regan, B.; Grätzel, M. *Nature* **1991**, *353*, 737–740.

surface−molecule interactions and ET dynamics at a single-molecule level. Ensemble-averaged ultrafast spectroscopy and single-molecule spectroscopy are complementary approaches for a fundamental understanding of interfacial electron transfer (IET) dynamics and related mechanisms. With a high temporal resolution, femtosecond transient absorption spectroscopy has been widely used to study ultrafast photoinduced dynamics in dye-sensitized TiO_2 nanoparticle (NP) systems.[9–11,23,30,57,58] By monitoring ground-state bleaching and recovery, the IET dynamics associated with intermediate states' formation and decay at the ensemble level can be investigated. Single-molecule spectroscopy,[14,35,41,47,59–65] involving fluorescence imaging and time correlated photon-stamping technique, has been demonstrated to be a powerful approach to investigate the inhomogeneous IET dynamics in heterogeneous systems. The IET dynamics have been found to be inhomogeneous, and the BET dynamics show multiexponential[11,12,20,66] or stretched exponential[8,17,46,67,68] behaviors due to the complexity of the local environment.

In our previous reports,[2,14,69] IET dynamics of Coumarin 343/TiO_2 and ZnTCPP/TiO_2 systems were studied at the single-molecule level on the basis of the fluorescence fluctuation dynamics arising from the IET activity fluctuation and intermittency. In this work, we systematically investigate the inhomogeneous IET dynamics of a 9-phenyl-2,3,7-trihydroxy-6-fluorone-sensitized TiO_2 NP system by combining ensemble-averaged femtosecond transient absorption spectroscopy and single-molecule photon-stamping measurements. Ultrafast FET (sub-picoseconds) and BET processes (picoseconds to tens of nanoseconds) are observed from ensemble-averaged ultrafast spectroscopy experiments. The inhomogeneous nature of the FET dynamics at the single-molecule level well explains the multiexponential dynamics measured in the ensemble experiments. The ET reactivity is dominated by the interactions between dye molecules and semiconductor NPs.

Experimental Section

Materials and Sample Preparation. 9-Phenyl-2,3,7-trihydroxy-6-fluorone (PF) and ethanol were purchased from Aldrich and used as received. TiO_2 NPs were prepared by hydrolysis of titanium isopropoxide as a precursor according to the literature protocol,[70] and the average size of TiO_2 NPs was 10−15 nm, determined by atomic force microscopy; thus, the calculated concentration of TiO_2 NPs was around 0.1 μM. For ensemble-averaged experiments, 100 μL of 1.0 mM PF in ethanol solution was added into a 2.0 mL TiO_2 NP solution in a quartz cuvette with 10 mm path length. The prepared sample was kept in a refrigerator for 12 h before the measurements in order to sufficiently incubate the PF and TiO_2 NPs mixture. The steady-state absorption spectra of PF and PF/TiO_2 solution were recorded by using a UV−visible spectrophotometer (Cary 50 Bio), and the steady-state emission of PF in ethanol solution was measured on a Felix32 fluorometer (Photon Technology International) with excitation at 518 nm. For single-molecule experiments, the sample preparation procedure has been reported in our previous work.[2,14] Briefly, for a control experiment, 25 μL of a 0.5 nM solution of PF in ethanol was spin-coated on a clean coverslip (Fisher, 18 mm × 18 mm, thickness ~170 μm) at 2000 rpm. The sample of PF on TiO_2 NPs for IET study was prepared by first spin-coating a 25 μL TiO_2 solution on a clean coverslip at 2000 rpm, followed by overlaying 25 μL of a 0.5 nM solution of PF in ethanol by spin-coating.

Femtosecond Transient Absorption. The femtosecond laser system for transient absorption measurements has been described

(22) Pan, D. H.; Klymyshyn, N.; Hu, D. H.; Lu, H. P. *Appl. Phys. Lett.* **2006**, *88*, 093121.
(23) Ramakrishna, G.; Singh, A. K.; Palit, D. K.; Ghosh, H. N. *J. Phys. Chem. B* **2004**, *108*, 1701–1707.
(24) Rochford, J.; Galoppini, E. *Langmuir* **2008**, *24*, 5366–5374.
(25) Tachikawa, T.; Cui, S. C.; Top, S.; Fujitsuka, M.; Majima, T. *Chem. Phys. Lett.* **2007**, *443*, 313–318.
(26) Tachikawa, T.; Fujitsuka, M.; Majima, T. *J. Phys. Chem. C* **2007**, *111*, 5259–5275.
(27) Verma, S.; Kar, P.; Das, A.; Palit, D. K.; Ghosh, H. N. *J. Phys. Chem. C* **2008**, *112*, 2918–2926.
(28) Kay, A.; Grätzel, M. *Chem. Mater.* **2002**, *14*, 2930–2935.
(29) Anderson, N.; Hao, E.; Ai, X.; Hastings, G.; Lian, T. *Physica E* **2002**, *14*, 215–218.
(30) Ramakrishna, G.; Ghosh, H. N. *Langmuir* **2004**, *20*, 7342–7345.
(31) Rath, M. C.; Ramakrishna, G.; Mukherjee, T.; Ghosh, H. N. *J. Phys. Chem. B* **2005**, *109*, 20485–20492.
(32) Rochford, J.; Chu, D.; Hagfeldt, A.; Galoppini, E. *J. Am. Chem. Soc.* **2007**, *129*, 4655–4665.
(33) Lee, J. K.; Ma, W. L.; Brabec, C. J.; Yuen, J.; Moon, J. S.; Kim, J. Y.; Lee, K.; Bazan, G. C.; Heeger, A. J. *J. Am. Chem. Soc.* **2008**, *130*, 3619–3623.
(34) Li, B.; Zhao, J.; Onda, K.; Jordan, K. D.; Yang, J. L.; Petek, H. *Science* **2006**, *311*, 1436–1440.
(35) Lu, H. P.; Xie, X. S. *J. Phys. Chem. B* **1997**, *101*, 2753–2757.
(36) Fox, M. A.; Dulay, M. T. *Chem. Rev.* **1993**, *93*, 341–357.
(37) Hoffmann, M. R.; Martin, S. T.; Choi, W. Y.; Bahnemann, D. W. *Chem. Rev.* **1995**, *95*, 69–96.
(38) McCusker, J. K. *Science* **2001**, *293*, 1599–1601.
(39) Joachim, C.; Ratner, M. A. *Proc. Natl. Acad. Sci. U.S.A.* **2005**, *102*, 8801–8808.
(40) Morfa, A. J.; Rowlen, K. L.; Reilly, T. H.; Romero, M. J.; van de Lagemaat, J. *Appl. Phys. Lett.* **2008**, *92*, 013504.
(41) Venkataraman, L.; Klare, J. E.; Nuckolls, C.; Hybertsen, M. S.; Steigerwald, M. L. *Nature* **2006**, *442*, 904–907.
(42) Whalley, A. C.; Steigerwald, M. L.; Guo, X.; Nuckolls, C. *J. Am. Chem. Soc.* **2007**, *129*, 12590–12591.
(44) Asbury, J. B.; Hao, E.; Wang, Y. Q.; Ghosh, H. N.; Lian, T. Q. *J. Phys. Chem. B* **2001**, *105*, 4545–4557.
(45) Gao, Y. Q.; Georgievskii, Y.; Marcus, R. A. *J. Chem. Phys.* **2000**, *112*, 3358–3369.
(46) Huber, R.; Moser, J. E.; Grätzel, M.; Wachtveitl, *J. Chem. Phys.* **2002**, *285*, 39–45.
(47) VandenBout, D. A.; Yip, W. T.; Hu, D. H.; Fu, D. K.; Swager, T. M.; Barbara, P. F. *Science* **1997**, *277*, 1074–1077.
(48) Warshel, A.; Parson, W. W. *Annu. Rev. Phys. Chem.* **1991**, *42*, 279–309.
(49) Lu, H.; Prieskorn, J. N.; Hupp, J. T. *J. Am. Chem. Soc.* **1993**, *115*, 4927–4928.
(50) Walters, K. A.; Gaal, D. A.; Hupp, J. T. *J. Phys. Chem. B* **2002**, *106*, 5139–5142.
(51) Yan, S. G.; Lyon, L. A.; Lemon, B. I.; Preiskorn, J. S.; Hupp, J. T. *J. Chem. Educ.* **1997**, *74*, 657–662.
(52) Liu, D.; Fessenden, R. W.; Hug, G. L.; Kamat, P. V. *J. Phys. Chem. B* **1997**, *101*, 2583–2590.
(53) Liu, D.; Kamat, P. V.; Thomas, K. G.; Thomas, K. J.; Das, S.; George, M. V. *J. Chem. Phys.* **1997**, *106*, 6404–6411.
(54) Myers, A. B. *Acc. Chem. Res.* **1997**, *30*, 519–527.
(55) Hupp, J. T.; Williams, R. D. *Acc. Chem. Res.* **2001**, *34*, 808–817.
(56) Hilczer, M.; Tachiya, M. *J. Phys. Chem. C* **2009**, *113*, 18451–18454.
(57) Ramakrishna, G.; Jose, D. A.; Kumar, D. K.; Das, A.; Palit, D. K.; Ghosh, H. N. *J. Phys. Chem. B* **2005**, *109*, 15445–15453.
(58) Anderson, N. A.; Lian, T. Q. *Annu. Rev. Phys. Chem.* **2005**, *56*, 491–519.
(59) Betzig, E.; Chichester, R. J. *Science* **1993**, *262*, 1422–1425.
(60) Lu, H. P.; Xie, X. S. *Nature* **1997**, *385*, 143–146.
(61) Lu, H. P.; Xun, L. Y.; Xie, X. S. *Science* **1998**, *282*, 1877–1882.
(62) Moerner, W. E.; Orrit, M. *Science* **1999**, *283*, 1670–1676.
(63) Schuler, B.; Lipman, E. A.; Eaton, W. A. *Nature* **2002**, *419*, 743–747.
(64) Trautman, J. K.; Macklin, J. J.; Brus, L. E.; Betzig, E. *Nature* **1994**, *369*, 40–42.
(65) Xie, X. S.; Dunn, R. C. *Science* **1994**, *265*, 361–364.
(66) Ghosh, H. N.; Asbury, J. B.; Weng, Y. X.; Lian, T. Q. *J. Phys. Chem. B* **1998**, *102*, 10208–10215.
(67) Nelson, J. *Phys. Rev. B* **1999**, *59*, 15374–15380.
(68) Nelson, J.; Haque, S. A.; Klug, D. R.; Durrant, J. R. *Phys. Rev. B* **2001**, *6*, 3–205321.
(69) Wang, Y.; Wang, X.; Lu, H. P. *J. Am. Chem. Soc.* **2009**, *131*, 9020–9025.
(70) Duonghong, D.; Borgarello, E.; Grätzel, M. *J. Am. Chem. Soc.* **1981**, *103*, 4685–4690.

in the literature.[71] Briefly, the laser pulses were generated at a 1 kHz repetition rate by a mode-locked Ti:sapphire laser (Hurricane, Spectra-Physics), and the pulse width was 110 fs. The output 800 nm pulse was split into pump and probe beams. The pump beam was sent into an optical parametric amplifier (OPA-800C, Spectra-Physics), and the output signal and 800 nm residual were mixed on a β-barium borate crystal to produce 518 or 480 nm light as the excitation source. The probe beam was delayed by a translation stage (MM 4000, Newport) and then focused into a rotating CaF_2 crystal to generate a white light continuum (wavelength ranging from 420 to 780 nm). An optical chopper was used to modulate the pump beam at 100 Hz, and the polarization orientation between pump and probe beams was set at the magic angle (54.7°). The pump and probe beams were overlapped on the magnetically stirring sample in a 10 mm path length cuvette, and then the continuum probe was coupled into a charge-coupled device spectrograph (Ocean Optics, S2000). The data acquisition and the delay control were programmed using LabVIEW (National Instruments) software. The instrumental response function is 0.25 ps at fwhm.

Single-Molecule Imaging and Photon-Stamping Measurements. The output of a mode-locked femtosecond Ti:sapphire laser (Coherent Mira 900D, 1.6 W, 200 fs fwhm, 76 MHz) was used to pump an optical parametric oscillator (APE-OPO, Coherent Inc.), and the output signal from the OPO was frequency-doubled to 528 nm by an LBO nonlinear optical crystal as the excitation source. The beam passed through a pair of prisms to eliminate the fundamental IR light and was then delivered into an inverted scanning confocal microscope (Axiovert 200, Zeiss) for single-molecule imaging and photon-stamping experiments. The beam was attenuated to 0.2−2.0 μW and sent into the microscope from its back side, reflected up by a dichroic beamsplitter (Z532rdc, Chroma), and focused by a 63×, 1.3 NA oil immersion objective onto the sample on a coverslip. The emission from the sample passed through a long-pass emitter (HQ545LP, Chroma) and a short-pass filter (FES0650, Thorlabs) and then was collected by a single-photon-counting avalanche photodiode (APD, Perkin-Elmer) for single-molecule imaging or by a Micro-Photon-Device (MPD, Picoquant) for single-molecule photon-stamping measurements. The photon stamping data were recorded by a time-correlated single-photon-counting (TCSPC) module (SPC-830, Becker & Hickl GmbH) at a FIFO mode, and the instrumental response function was 115 ps at fwhm.

Results and Discussion

Xanthene dyes and its derivatives, including PF, are widely used as sensitizers in dye-sensitized NP systems.[72−75] The excited state of the PF injects electrons into the conduction band or energetically accessible surface states of TiO_2 NPs under photon excitation, and the PF contains active OH groups that can anchor on the TiO_2 surface via chelation.[15,73,76,77] The steady-state absorption spectra of PF in ethanol and PF in TiO_2 colloid solution are shown in Figure 1A,B, and the emission of PF in ethanol is shown in Figure 1C. The absorption spectrum of PF in ethanol covers the wavelength range from 445 to 550 nm and peaks at 518 nm. As shown in Figure 1B, the

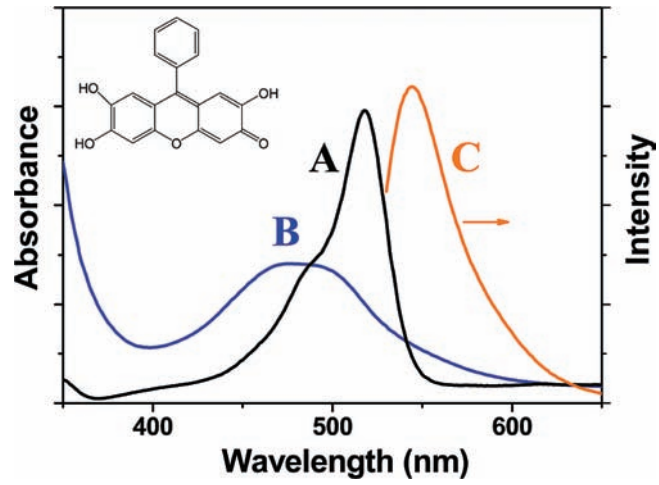

Figure 1. Steady-state spectra of 9-phenyl-2,3,7-trihydroxy-6-fluorone. (A) Absorption of PF in ethanol and (B) absorption of PF in TiO_2 NPs aqueous solution (pH = 2.8). The broadened and blue-shifted absorption spectrum of PF in TiO_2 NPs colloid solution indicates the existence of a charge-transfer interaction between PF and TiO_2 NPs.[79] (C) Emission spectrum of PF in ethanol. No emission of PF was observed in TiO_2 solution due to the efficient electron transfer to TiO_2 NPs. The inset shows the molecular structure of PF.

characteristics of the absorption spectrum of PF/TiO_2 solution are (1) the prominent blue shift of the absorption maximum, (2) a broad absorption band around 475 nm, and (3) a significant absorption decrease at 518 nm compared to the spectrum of PF alone in ethanol. Evidentially, the orange color of the PF in ethanol becomes reddish in TiO_2 aqueous solution, indicating a strong ground-state electronic interaction and IET between PF and TiO_2.[15,78,79] Accordingly, the emission of PF in TiO_2 solution disappeared and could not be detected in our measurements. These observations are consistent with the literature and can be interpreted on the basis of the high polarity of the TiO_2 surface and the formation of a new charge-transfer state due to the strong coupling between PF and TiO_2 NPs via chelation.[76,77]

To get a deeper insight into the fundamental IET mechanisms of the PF/TiO_2 system, we conducted femtosecond transient absorption measurements. Figure 2 shows the transient absorption spectra of PF/TiO_2 solution at 0.5, 2.0, 20, and 500 ps delay times with excitation at 518 nm. It is obvious that the profile of negative signal from 420 to 520 nm is similar to the steady-state absorption spectrum of the PF/TiO_2 solution (Figure 1), reflecting the ground-state bleaching dynamics. For a strongly coupled dye/TiO_2 system, a new charge-transfer complex could be formed and can be experimentally evidenced by the occurrence of a new band in the absorption or emission spectrum.[9,20,73] From our control measurement for PF in ethanol, no similar absorption features are observed in this frequency domain, so a contribution from excited singlet or triplet states of PF is

(71) Nikolaitchik, A. V.; Korth, O.; Rodgers, M. A. J. *J. Phys. Chem. A* **1999**, *103*, 7587–7596.
(72) Pelet, S.; Grätzel, M.; Moser, J. E. *J. Phys. Chem. B* **2003**, *107*, 3215–3224.
(73) Ramakrishna, G.; Ghosh, H. N. *J. Phys. Chem. B* **2001**, *105*, 7000–7008.
(74) Jhonsi, M. A.; Kathiravan, A.; Renganathan, R. *J. Mol. Struct.* **2009**, *921*, 279–284.
(75) Sayama, K.; Sugino, M.; Sugihara, H.; Abe, Y.; Arakawa, H. *Chem. Lett.* **1998**, *27*, 753–754.
(76) Frei, H.; Fitzmaurice, D. J.; Grätzel, M. *Langmuir* **1990**, *6*, 198–206.
(77) Mosurkal, R.; He, J. A.; Yang, K.; Samuelson, L. A.; Kumar, J. *J. Photochem. Photobiol. A* **2004**, *168*, 191–196.
(78) Rehm, J. M.; McLendon, G. L.; Nagasawa, Y.; Yoshihara, K.; Moser, J.; Grätzel, M. *J. Phys. Chem.* **1996**, *100*, 9577–9578.
(79) The PF−TiO_2 absorption spectrum changes under certain contributions, including ground electronic coupling between electron donor and acceptor, solvent mediation, protonation/deprotonation, and so on. The observed absorption spectrum in this work also shows a pH dependence and blue-shift with a decrease in the pH value. Due to the strong interaction between PF and TiO_2, the excited state and/or the ground state of PF in TiO_2 solution would be shifted up/down compared with that of PF in ethanol. The broadened absorption band of PF indicates the inhomogeneous interaction covering strong and weak electronic coupling cases. The results of our measurements are consistent with the results reported in ref 78.

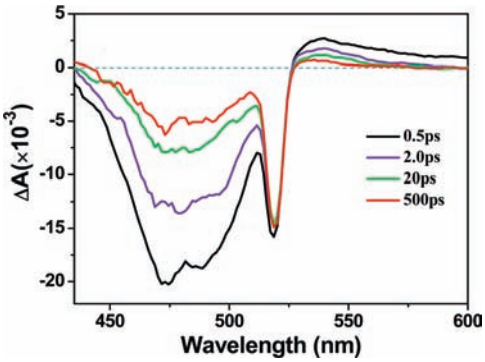

Figure 2. Transient absorption spectra of PF in TiO_2 NP aqueous solution at 0.5, 2.0, 20, and 500 ps delay times, with pulse excitation at 518 nm. The spectrum at each time delay consists of a broad ground-state bleaching from 420 to 520 nm and a positive broad charge separation band with a maximum at 540 nm. The group velocity dispersion of the probe light and spectral signal was already considered when constructing the time-resolved spectra.

precluded. Thus, the positive transient absorption band peaking at 540 nm (Figure 2) is assigned to a charge separation/charge-transfer state of $PF^{\delta+}-TiO_2^{\delta-}$.

Experimentally, charge separation and FET processes can be observed, and their rates can be deduced from time-resolved transient absorption signal traces, whereas BET dynamics can be measured by the ground-state absorption bleaching recovery of the sensitizer or by the decay of transient absorption from the intermediate charge-transfer state. Figure 3A shows the transient traces, probed at 540 nm, of the charge-transfer state $PF^{\delta+}-TiO_2^{\delta-}$ within short and long delay-time windows. A rise and two decay exponential components were observed from the transient dynamics. The rise component, with a 0.4 ± 0.1 ps time constant, is attributed to the formation process of the charge separation state. We attribute the two decay components, with 3.0 ± 0.1 ps (82%) and 11.5 ± 0.5 ns (18%) time constants, to two typical channels of the charge recombination process. Specifically, the ultrafast 3.0 ps component is attributed to the charge recombination (BET) process for a strong PF/TiO_2 coupled condition.[78,79] On the other hand, at PF concentration of ~0.05 mM under our experimental conditions, it is possible for some PF molecules to adsorb on the TiO_2 surface with a weak PF/TiO_2 coupling that gives rise to the slow component of the BET dynamics. This attribution is well supported by the results from monitoring the ground-state bleaching recovery at 455 nm (Figure 3B). By fitting the transient traces at 455 nm, two exponential components, 3.0 ± 0.1 ps (84%) and 11.5 ± 0.5 ns (16%), were obtained. Unambiguously, both the time constants and the corresponding weights of the fast and slow exponential components are consistent with the probed BET dynamics measured by transient absorption from the charge-transfer state or ground-state bleaching recovery. Similar results of ultrafast electron injection and charge recombination, including both fast and slow BET processes, were also reported in other dye-sensitized TiO_2 systems.[57]

Based on the above ensemble-averaged spectroscopy measurements, two types of electron-transfer channels between PF and TiO_2 NPs are probed. From the steady-state absorption spectrum (Figure 1), the broadened and blue-shifted absorption band with a maximum around 475 nm demonstrates the existence of a strongly coupled PF/TiO_2 state, implying that the distribution of energy gap between excited singlet and ground states is larger for the new charge-transfer complex PF/TiO_2 than that for PF dye alone.[78,79] The strong interaction

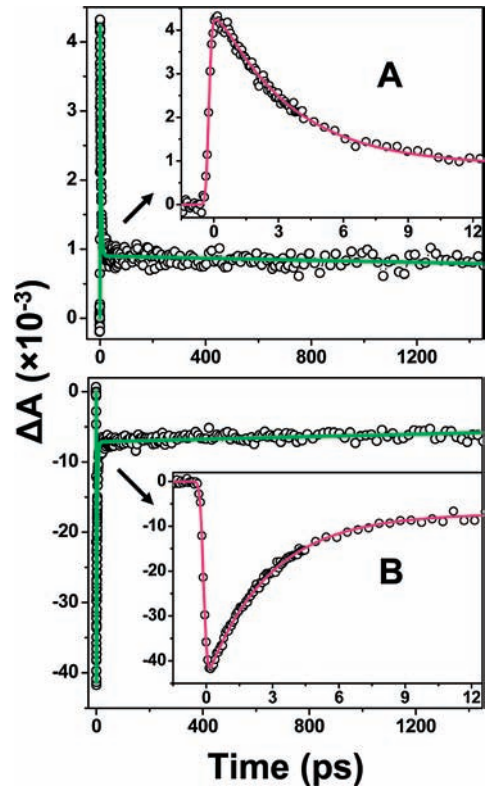

Figure 3. Transient spectral traces of ensemble-averaged ultrafast spectroscopy measurements on the interfacial electron transfer dynamics of the PF/TiO_2 NP system. (A) Charge separation state at 540 nm of PF/TiO_2 in a long and short time windows, with excitation at 480 nm. Three components are obtained by fitting this trace: one rise component with time constant 0.4 ± 0.1 ps, and two decay components with time constants 3.0 ± 0.1 ps (82%) and 11.5 ± 0.5 ns (18%). (B) Ground-state bleaching recovery at 455 nm in a long and short time windows, with excitation at 480 nm. Two components were observed: 3.0 ± 0.1 ps (86%) and 11.5 ± 0.5 ns (14%), reflecting two backward electron-transfer rates and channels.

between donor (PF) and acceptor (TiO_2) enables the excited state of PF to inject an electron directly within 0.4 ps into a new localized state formed between PF and TiO_2. Accordingly, the BET process also shows ultrafast dynamics with a time constant of 3.0 ps for the strongly coupled PF/TiO_2. The physical nature of the ultrafast ET process is a charge-transfer transition excitation.[50] However, for the weakly coupled PF/TiO_2, the electron could be injected via the excited state of PF into the conduction band or energetically available surface states of TiO_2 and then recombine with the ground state of PF through a BET rate process, most likely involving in excess electron non-Brownian motions or scattering processes in TiO_2 NPs. This BET process takes a longer time, from sub-nanoseconds to milliseconds, which was also reported in other similar dye-sensitized TiO_2 NP systems.[8,20,23,43] Due to the complex nature, multiexponential or stretched exponential IET dynamics is typically observed in ensemble-averaged experiments, such as in our transient absorption measurements discussed here.[11,12,49,52,66] This complexity can be further explored and analyzed by single-molecule experiments, which has demonstrated that the IET reactivity often shows intermittency and fluctuations.[2,35]

Figure 4A,B shows the single-molecule fluorescence images of PF on a glass coverslip and a coverslip coated by TiO_2 NPs under the same experimental imaging conditions, respectively. Comparing the detectable signal for PF molecule density in the two images, it can be seen that the molecule density in a frame of PF imaged on TiO_2 is less than that of PF on a coverslip.

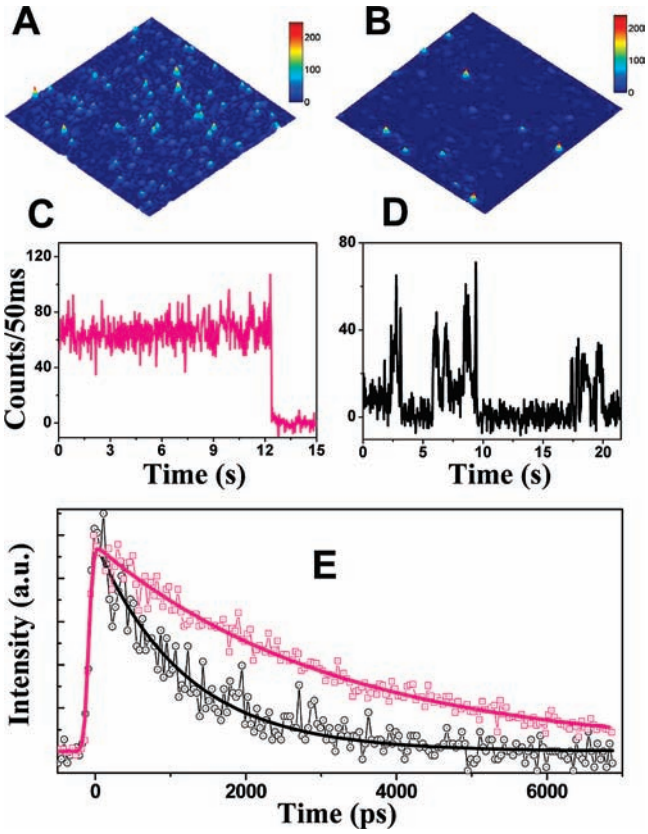

Figure 4. (A,B) Single-molecule images of PF on a glass coverslip and on a TiO_2 NPs-coated surface (size: 20 × 20 μm), respectively, obtained under the same experimental imaging conditions. (C,D) Typical fluorescence trajectories of single-molecule PF on a glass coverslip and on a TiO_2 NPs-covered surface, respectively, with the binning time of 50 ms. (E) Typical fluorescence emission traces of single-molecule PF on a coverslip (pink) and on a TiO_2 NPs-coated surface (black), using single photon stamping recording with the pulse laser excitation at 528 nm and 200 fs. Single exponential decay is observed with a 3.2 ± 0.1 ns lifetime of PF on the coverslip and 1.2 ± 0.1 ns on the TiO_2 NPs-covered surface.

The remarkable fluorescence quenching of PF on TiO_2 indicates the electron transfer occurring at the PF/TiO_2 NP surface at a single-molecule level, which is consistent with the steady and transient absorption data. Presumably, a single molecule should not be optically visible if the molecule is electronically strongly coupled with TiO_2 or involved in a high ET-activity state. In contrast, a weakly coupled PF/TiO_2 system would be optically visible in our single-molecule imaging measurements and demonstrate fluorescence intensity fluctuation because the system fluctuates between higher ET-activity states and lower ET-activity states.Figure 4C,D shows the single-molecule emission trajectories for PF on glass and on TiO_2 NP surfaces (binning time, 50 ms), respectively. The fluorescence trajectory of PF on TiO_2 (Figure 4D) shows a strong fluctuation with respect to a relatively stable emission on a glass surface (Figure 4C). Similar single-molecule fluorescence intensity fluctuations were also observed in our previous works on Coumarin 343/TiO_2 and ZnTCPP/TiO_2 systems.[2,14] The dark state reflects the IET process quenching the emission of PF with a high ultrafast ET activity, and the bright state is due to the low activity of ET and the emission associated with the radiative relaxation from excited state to ground state. The ET-activity of optically visible PF/TiO_2 NP systems is monitored by single-molecule fluorescence lifetime fluctuation. From the lifetime data, we get the FET from PF to TiO_2 NPs. Figure 4E shows two typical

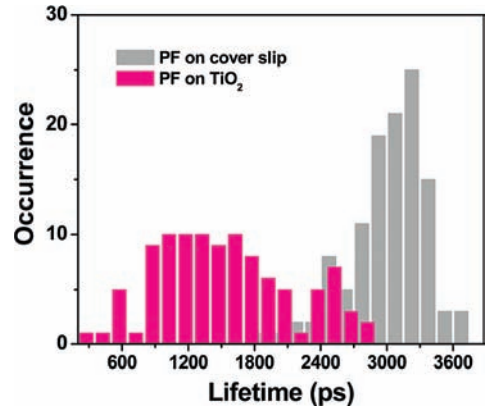

Figure 5. Fluorescence lifetime distribution of PF on a glass coverslip surface (gray) and on a TiO_2 NPs-coated surface (pink). A narrow distribution ranging from 1.8 to 3.8 ns with 550 ps fwhm for PF on glass, and a wide distribution from ~200 ps to 2.9 ns with 1.3 ns fwhm for PF on TiO_2 NPs surface, are obtained within our instrumental limits.

single-molecule fluorescence decay curves for PF on the glass surface and on a TiO_2 NPs-covered surface, respectively. Both transient signals are fitted with single exponentials, and the fitted time constants are 3.2 ± 0.1 ns for PF on the glass coverslip and 1.2 ± 0.1 ns for PF on the TiO_2 NP surface. As mentioned earlier, the fluorescence quenching is attributed to interfacial FET from the excited states of the adsorbate PF to TiO_2 NPs.

The IET rate is highly sensitive to the interactions between the adsorbate molecules and TiO_2 NPs. Due to the inhomogeneous nature of the interactions from molecule to molecule, the lifetime or the FET rate is expected to be inhomogeneous, which has also been demonstrated in previous publications for similar dye-sensitized IET systems.[35] Figure 5 shows the single-molecule fluorescence lifetime distributions for single-molecule PF on glass coverslips and on TiO_2 NPs-covered surfaces. The lifetime of PF on glass coverslips in a control experiment shows a narrow distribution range (from 1.8 to 3.8 ns) with a 550 ps fwhm. In contrast, for PF molecules on TiO_2 NPs, a wide distribution of fluorescence lifetime is obtained, ranging from ~200 ps to 2.9 ns with a 1.3 ns fwhm. Unfortunately, we cannot measure a single-molecule lifetime shorter than 200 ps due to the limited sensitivity for imaging and time resolution of the instrumental response. However, it could be extrapolated that there is a much wider lifetime distribution down to picoseconds or sub-picoseconds for the PF/TiO_2 NP system. The lifetime distribution clearly demonstrates the inhomogeneous interfacial FET rate and is consistent with the attribution of ET reactivity fluctuation dynamics, which can be revealed by the single-molecule experiments but not by the ensemble-averaged measurements.

Single-molecule spectroscopy and ensemble-averaged transient absorption measurements provide powerful "zoom-in" and "zoom-out" views of the IET dynamics of the PF/TiO_2 system. The ultrafast FET processes deduced from the ensemble-averaged transient absorption spectroscopy are precisely projected to a wide time window revealed by our single-molecule lifetime measurements. In the PF/TiO_2 system, the ET rate is dominated by the electronic coupling between PF and TiO_2: and the ultrafast FET corresponding to the strong coupling can be observed from ensemble-averaged transient absorption dynamics, and the relatively slower FET corresponding to the relatively weaker coupling can be demonstrated by single-molecule fluorescence photon-stamping measurements (Figure 4). On the other hand, the biexponential BET dynamics can be

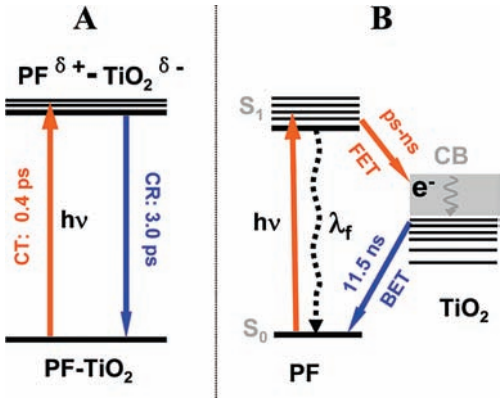

Figure 6. Schematic diagrams showing two typical electronic couplings and two typical cases of interfacial electron transfer in a PF/TiO_2 system. (A) Strong electronic coupling channel. PF−TiO_2 and $PF^{\delta+}$−$TiO_2^{\delta-}$ are the ground state and the charge transfer state, respectively. CT, charge transfer; CR, charge recombination. (B) Weak electronic coupling channel. S_0 and S_1 are the ground state and excited state of PF in TiO_2 colloids solution, respectively. CB, conduction band; FET, forward electron transfer; BET, backward electron transfer.

interpreted by the inhomogeneous ET performance revealed in the single-molecule measurements.

On the basis of the biexponential characteristics of the BET dynamics and the deduced two typical charge recombination processes (Figure 3), we propose a model consisting of two different IET channels to characterize the FET and BET reactions in the ET dynamics of the PF/TiO_2 system. Figure 6 shows the schematic diagrams of the IET in PF/TiO_2 system for two typical interactions, strong coupling and weak coupling. PF−TiO_2 and $PF^{\delta+}$−$TiO_2^{\delta-}$ in Figure 6A represent the ground state and charge separation states for a strongly coupled PF/TiO_2 system, and S_0 and S_1 in Figure 6B are the ground state and the singlet excited state of PF for weakly coupled PF/TiO_2. In the strongly coupled state, under photon excitation, the electron state of PF−TiO_2 is directly transferred into the $PF^{\delta+}$−$TiO_2^{\delta-}$ charge separation state within 0.4 ps, similar to the intramolecular FET such as charge separation in metal-to-ligand charge-transfer processes.[16,50,80] The charge-transfer process can be monitored on the basis of the formation of a charge separation state at 540 nm in the transient absorption measurements. The 3.0 ps charge recombination time was obtained from the recovery of ground-state bleaching and the decay of the charge separation state. At the single-molecule level, the location of the charge-transfer state, the charge-transfer rate, and the charge recombination rate are inhomogeneous. In the weakly coupled PF/TiO_2 system, the electron of PF is injected into the conduction band or energetically accessible surface state via its excited singlet state (see Figure 6B). This forward electron injection takes picoseconds to nanoseconds, depending upon the interaction of individual PF/TiO_2 events; the excited state of PF is shown as electron-transfer singlet states in Figure 6B. After injection, the electron presumably undergoes trapping and detrapping and non-Brownian motions or scattering in TiO_2 NPs and then recombines with the cation $PF^{\delta+}$. The BET process takes tens of nanoseconds up to sub-microseconds, which is demonstrated by transient absorption spectroscopy. We conclude that the fluorescence blinking/ET-activity fluctuation and the lifetime distribution of single-molecule PF/TiO_2 demonstrate an inhomogeneity of interfacial FET dynamics, originated from the inhomogeneous interactions between PF and TiO_2 NPs.

The characteristics of IET dynamics, such as the high inhomogeneity of the dynamics revealed at the single-molecule level and multiexponential dynamics in the ensemble measurements, are dominated by the inhomogeneous interactions between the dye molecules and the semiconductor TiO_2 NPs. The primary parameters of the interactions include the driving force of the free energy gap between the electron-transfer donor and acceptor, the vibrational relaxation energy of dye molecules and surface vibrational modes of TiO_2, and the related electronic coupling between the electron transfer donor and acceptor. All of these factors are determined by the chemical and physical nature of both dye molecules and semiconductor NPs and can also be perturbed by local environments. Our understanding is also consistent with the previous reports, which suggest that surface defects,[81] distribution of donor−acceptor distance,[82] and multiple time scales of solvent dynamics are possible reasons for the complex IET dynamics.[83] The inhomogeneous interactions reflected by complex ET dynamics showing broad distributions can be probed complementarily by both single-molecule spectroscopy measurements and transient ensemble-averaged spectroscopy measurements. To get further insight into the IET dynamics and to probe the interactions between dye molecules and semiconductor NPs, we have applied Raman spectroscopy to probe the reorganization energy of the IET,[22,84] and recently, ultrafast exciton dynamics studies also demonstrated a possible way to probe the ultrafast ET dynamics at the single-molecule level.[85,86]

Conclusion

Interfacial electron transfer dynamics of 9-phenyl-2,3,7-trihydroxy-6-fluorone (PF)-sensitized TiO_2 nanoparticles has been probed by combined single-molecule photon-stamping spectroscopy and femtosecond transient absorption spectroscopy. At the single-molecule level, the ET dynamics were found to be inhomogeneous, indicating the inhomogeneous electronic coupling and ET activity in the PF/TiO_2 system. The inhomogeneous nature of the ET dynamics revealed by the single-molecule technique suggests the multiexponential ET dynamics measured in ensemble-averaged experiments. Based on the transient and static absorption spectroscopy, two types of molecular interactions, strong coupling and weak coupling, are demonstrated to coexist between PF molecules and TiO_2 NPs, and a two-channel mechanism is proposed to interpret the observed interfacial ET dynamics. The inhomogeneous electron transfer rate due to the interaction between a dye molecule and the semiconductor surface depends on the chemical and physical nature of both the dye molecule and the semiconductor.

Acknowledgment. We acknowledge our use of the facility of the Ohio Laboratory for Kinetic Spectrometry of the Center for Photochemical Sciences at BGSU for our ensemble-averaged femtosecond transient spectroscopy measurements. This work is supported by the Office of Basic Energy Sciences within the Office of Science of the U.S. Department of Energy (DOE).

JA909168E

(80) Benkö, G.; Kallioinen, J.; Korppi-Tommola, J. E. I.; Yartsev, A. P.; Sundström, V. *J. Am. Chem. Soc.* **2002**, *124*, 489–493.
(81) Bell, T. D. M.; Pagba, C.; Myahkostupov, M.; Hofkens, J.; Piotrowiak, P. *J. Phys. Chem. B* **2006**, *110*, 25314–25321.
(82) Murata, S.; Tachiya, M. *J. Phys. Chem. A* **2007**, *111*, 9240–9248.
(83) Bixon, M.; Jortner, J. *Adv. Chem. Phys.* **1999**, *106*, 35–202.
(84) Pan, D. H.; Hu, D. H.; Lu, H. P. *J. Phys. Chem. B* **2005**, *109*, 16390–16395.
(85) Hernando, J.; van Dijk, E.; Hoogenboom, J. P.; Garcia-Lopez, J. J.; Reinhoudt, D. N.; Crego-Calama, M.; Garcia-Parajo, M. F.; van Hulst, N. F. *Phys. Rev. Lett.* **2006**, *97*, 216043.
(86) Min, W.; Lu, S.; Chong, S.; Roy, R.; Holtom, G. R.; Xie, X. S. *Nature* **2009**, *461*, 1105–1109.